

Practical capabilities of MFL in steel plate inspection

Neil R. PEARSON^{1,2}, Matthew A. BOAT¹, Robin. H. PRIEWALD², Matthew J. PATE^{1,2}, John S. D. MASON²

¹Silverwing UK Ltd; Unit 31 Cwmdru Industrial Estate, Swansea, SA5 8JF, UK; e-mail: npearson@silverwinguk.com

²College of Engineering, Swansea University, Singleton Park, Swansea, SA2 8PP, UK

Abstract

Magnetic flux leakage (MFL) is a widely used approach to detect corrosion in applications where large areas are to be inspected in short time scales. A particularly good example is in above ground storage tanks (ASTs) within the petrochemical industry where tank floors are inspected periodically, calling for the AST to be taken out-of-service and emptied. This makes maintenance times that much more expensive and calls for techniques that are both reliable and fast. MFL is widely used in the context because of its inherent speed.

Magnetic flux leakage (MFL) is a widely used and accepted technology for locating defects on a tank floor. While MFL signals are often linked to the volume of a defect, its depth is perhaps the most difficult to estimate and the most critical dimension since it indicates the closeness of a potential leak and if misinterpreted can lead to erroneous repair strategies with costly outcomes. Therefore, accurately determining the geometry of defects is pivotal if an optimum repair strategy is to be formulated.

In this paper we look to understand why these relationships occur and attempt to minimise them by characterising the influence of two fundamental components of the defect geometry, namely the length and depth. Analysis of the corresponding MFL signals leads to a novel, multi-valued reference map which is capable of reducing the depth error by around 40 %.

Keywords: Magnetic flux leakage (MFL), defect characteristics, defect normalisation, defect geometry.

1. Introduction

In 1988 Saunderson [1] was tasked with improving the probability of detecting corrosion defects on the floors of above ground storage tanks (ASTs). Prior to Saunderson, the practice of floor inspection involved obtaining sample spot ultrasonic (UT) thickness measures over the whole floor area in a sparse grid-like pattern. By its very nature, manually sampling by UT is a time consuming approach and it is reported in [1] that for an AST of 25m in diameter, the acceptable coverage would require 1.6 million spot measures. To improve the inspection strategy, Saunderson [1] proposed magnetic flux leakage (MFL) as a viable alternative. With an array of non-contact magnetic sensors, Saunderson comments that the key benefit of the MFL approach is the ability to cover a large percentage of floor area quickly.

While a system based on MFL is able to perform a rapid survey of the AST floor, the signals received from the corresponding defects can prove difficult to interpret. One reason for this difficulty is that MFL signals are found to be *“more closely related to volume of metal loss than to the depth of pitting”* [1]. Unfortunately, a volumetric measurement, although of some value, is in itself insufficient. For example, a narrow pipe shape defect with a relatively small volume can prove far more costly than a broad, flatter lake shape defect with a larger volume. It follows that a critical component is the depth of a defect [2].

Realising the importance of defect depth, Saunderson [1] proposed a serial approach: to first screen the floor for defects followed by a detailed inspection of suspect locations. Saunderson suggested that MFL based inspections should be supplemented with *“manual UT for validation and residual thickness measurement”* in order to obtain the necessary information to determine repair strategies, a procedure that is still today considered best practice in the UK [3]. However, the second stage UT validation clearly increases the out-of-service period and therefore costs.

Following the original screening tool developed by Saunderson [1], much research in the field of MFL, including that in the context of pipeline inspection, has been aimed at quantifying defect characteristics with greater accuracy. The ultimate goal is to map MFL signals back to their corresponding defect shapes. Various approaches have

attempted to address the problem of translating MFL signals into good, reliable representations of the defect, these approaches are generally referred to as *defect reconstruction*. These approaches exhibit a trade-off between computational efficiency and accuracy of the reconstructed profile. Three primary categories can be considered under the umbrella of defect reconstruction, namely *defect referencing*, *classification* and *inverse modelling*. Arguably, this list can be ordered from low to high in terms of defect profile accuracy and in terms of efficient computation from high to low.

1.1. Defect referencing

Referencing scales the MFL signals in a suitable manner allowing for an estimate of the corresponding defect geometry. Several publications, for example [4–10] have analysed the defect geometries in terms of their width, length and depth and report a complex relationship between these dimensions and corresponding MFL signals.

In 1995, observations by Charlton [4] led to a simple defect characterisation approach. Charlton collects information from a set of pre-defined and emulated defects to create a lookup table of reference scans (also referred to as calibration curves) that are then used to scale subsequent MFL signals. In the context of ASTs, the set of emulated defects is normally designed to emulate the natural and uniform growth of corrosion; i.e. where the surface area grows proportionally as the depth of the defect increases [5, 6]. However, the accuracy of the calibration curve is dependent upon the accuracy of the emulations including the chosen volume and shape [1] and their ability to truly represent the scope of possible corrosion. As such, this simple form of referencing is inherently limited as it is unable to accurately scale MFL signals over the continuum of defect geometries.

In 1999, the relationship between MFL signals and the length of corresponding defects was studied by Siebert and Sutherland [7]. They report that over a limited range of geometries, the horizontal (or lateral) distance between the positive and negative peaks of the normal component of the MFL signal gives a reliable and “*crisp definition of defect length*”. Furthermore in 2004 Huang et al. [8] reported that the amplitude of the MFL signal increases in a linear fashion as the length of the defect grows. In these cases, both the width and depth were normalised. However, for reasons which are unclear, the lengths examined were between 2 mm and 16 mm only. A larger and more complete analysis would need to be performed to corroborate the linear relationship.

The non-trivial task of ascertaining the defect geometry is illustrated well by Qi et al. in 2006 [9]. From a limited set of defects, they remarked that the three independent defect dimensions were a function of the MFL signal:

- Width: Increasing the width of a defect can increase the amplitude of the received MFL signal.
- Length: The peak amplitude of the MFL signal increases in a near-linear fashion as the length of the defect increases. This finding is in accord with that of Huang et al. [8] from 2004, however Qi et al. [9] furthered the investigation and found that as the range of the defect length increased the amplitude of the received MFL signal reaches a steady-state when the defect length is above 30 mm.
- Depth: In 2006 Qi et al. [9] concluded that the most critical of the three dimensions, namely depth, is also the most difficult to establish as:
 1. The MFL amplitude tends to increase in a non-linear manner as the depth of the defect increases and
 2. The amplitude of the MFL signal varies in a non-linear fashion when both the width and length components are varied and the depth is kept constant. This makes estimating the depth from the amplitude alone difficult unless the width and length parameters are established first.

More recently in 2010, further attempts to better estimate the shape, in particular the defect depth have been made by Saha et al. [10]. In the context of pipeline inspection, Saha et al. established a better depth estimate by considering the influence of the defect width. In [10], it is reported that “*estimation [of the depth] is very sensitive to the width of the defect and a good estimate of width is essential for proper depth sizing*”. While this outcome was observed earlier by Qi [9], Saha et al. demonstrates an interesting approach to ascertain a defect width by using only the radial (Y) component of the MFL signal from a linear array of sensors. In conjunction with an estimate of the defect length, Saha et al. proposes a second order relationship to establish the defect depth. However, the proposed function does portray limitations in that it is “*predominantly a linear function of the [width/length]*” [10], a linear function that seems to contradict the ‘non-linear’ relationship reported by Qi et al [9].

While the referencing approach in its present form does not provide very accurate representations of defect geometries, its efficiency in terms of immediate reporting is beneficial. One possible avenue to enhance the accuracy of the reported geometry is *classification*, the second general category of MFL analysis.

1.2. Classification

Classification operates on characteristics obtained from a collection of features from MFL signals which are normally compared in a statistical manner to a closed set of pre-defined reference models. Classification has two necessary stages namely, training and testing. Applicable to both are the features, based for example on the aforementioned geometric measures or through holistic means [11]. The training comprises of representative models trained on known classes, see for example [12]. The testing stage is the classification task itself, i.e. the scoring method based on, for example, neural networks [13] or support vector machines [14, 15]. We can observe that publications, e.g. [11] tend to concentrate on the former; improving the feature extraction process while standard and readily available classifiers are used to calculate the likelihood of the defect category.

Classification has two distinct applications in the context of MFL inspection. The first is to categorise defects into higher-level subsets e.g. pipe, conical or lake type shapes as proposed by Ramirez [14] and the second avenue involves defect reconstruction through classification, i.e. postulate the defect geometry [16]. Reported work in [16] to reconstruct defects with classification has successfully demonstrated its worth, with rates of up to 99 % accuracy but these results are based on a controlled and constrained set of emulated defects.

1.3. Inverse modelling

The third category of MFL analysis is *inverse modelling*. Inverse modelling aims to provide the ideal solution: the reconstruction of a detailed profile of the corresponding defect from received MFL signals. This approach is deemed to “*potentially provide a powerful means of the detection and characterisation of defects in MFL data analysis*” [17]; a view expressed by others [18–20].

The basic principle of inverse modelling is to iteratively adapt a forward model so that a surface profile of the defect is generated. With a theoretically computed forward model and a corresponding unknown MFL signal, a comparison can be made. If the modelled and unknown MFL signals are dissimilar, parameters of the forward model are adapted in an attempt to move the forward model closer to simulating the original surface profile. This cycle is iterated until the computed and measured signals meet some user defined convergence criteria. A conventional iterative numerical modelling approach is the accurate, albeit computationally expensive finite element model [18].

Much of the current research into inverse modelling aims to improve the computational efficiency of the forward model whilst maintaining the accuracy of defect reconstruction. At present and due to the iterative nature of inverse modelling, the demands placed upon computing make it a potentially very expensive, non-viable option for field use where the locations of ASTs can be both remote and hostile and where time is usually an important economic factor. If a computationally efficient process could be devised then inverse modelling appears to be a most promising approach. A possible route towards a more computationally efficient inverse modelling approach whilst maintaining relatively high accuracy of the defect profile is the use of a ‘particle filter’ in place of the complete finite element model [21]. Other attempts to increase the efficiency of inverse modelling include substitution of a stochastic modelling in the form of neural network classifiers [16, 22], wavelets [23] and statistical classifiers [24]. It could be argued that inverse modelling appears to have a bright future but we need to establish a better approach coupled with tomorrows portable technologies.

In this paper we forgo the advanced and as yet non-viable inverse modelling approach and propose an improved, in terms of accuracy, ‘defect referencing’ approach, using complementary information extracted from the MFL signal that estimates of the length and depth of the corresponding defects.

2. Signal acquisition and the shapes of defects

The basic principle of inspecting a ferrous specimen with MFL firstly involves suitably saturating the local area of interest with a magnetic field. In the vicinity of a defect, the reluctance to the induced magnetic field increases and if high enough, the induced magnetic field will diverge around the absence of material. This field can diverge around the

defect both within the surrounding material and also ‘leak’ outside its confines. The quantity of the leaking magnetic field, deemed proportional to the volume of the defect [1], is then measured by suitably placed magnetic sensors.

To perform a rapid inspection of an AST floor, a scanner with a linear array of sensors is normally used and orientated perpendicularly to the direction of travel so that an area can be covered with one sweep. In this work, MFL signals are considered as if received from a single magnetic sensor and have been generated via a magneto-static 2D finite element modelling.

Furthermore a homogeneous magnetic field is assumed with a pre-determined magnetic field strength fixed to achieve the suitable saturation of a 6 mm steel plate; the homogeneous field is such that it is fixed in the plate at two Tesla. All MFL signals in this paper are extracted 3.8 mm above the top surface of the specimen and orientated to collect the Y component of the magnetic flux density \vec{B} (where $\vec{B} = (B_x, B_y, B_z)$) at equidistant points across the surface of the specimens. Only rectangular profiles are considered, allowing the geometric depth or length to be adjusted readily and independently.

3. Influence of defect characteristics on MFL signal

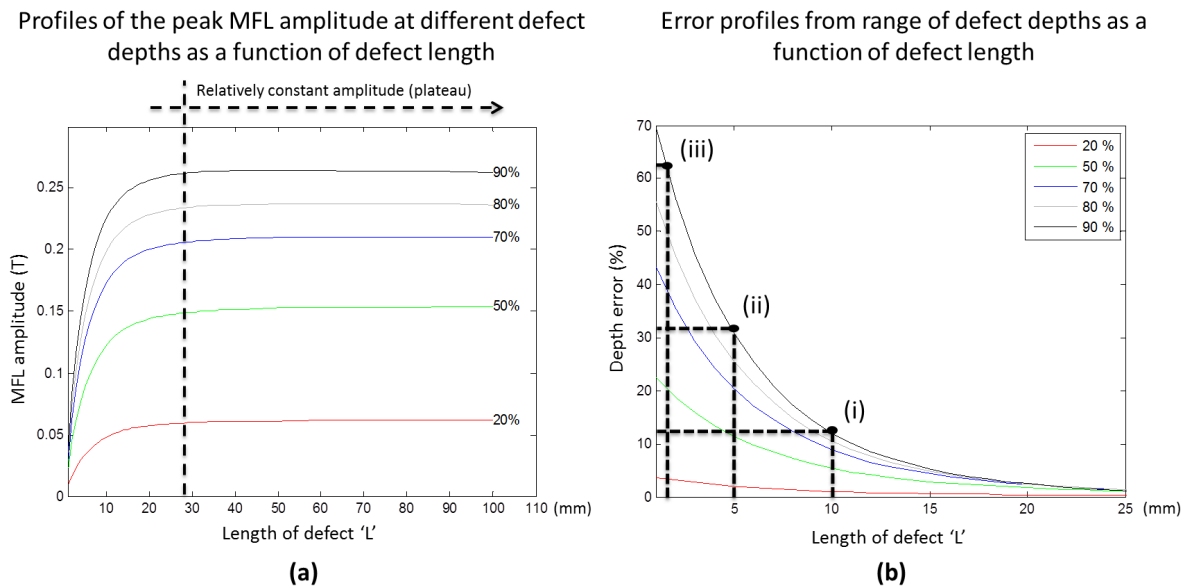


Figure 1: (a): Five profiles from rectangular defects of depth 20 %, 50 %, 70 %, 80 % and 90 % reflecting the peak MFL signal amplitudes. Each profile is a function of a rectangular defect varying in length ‘L’ from 1 mm and 100 mm. (b): The potential deviation of the MFL depth estimate from the true defect depth as a function of defect length ‘L’. The highest error rates are found in narrow defects. The error above the maximum range of ‘L’ shown on the abscissa remains close to zero.

In Figure 1(a) the peak amplitude of MFL signals as a function of the defect length ‘L’ is presented. Rectangular defect of uniform depths ‘d’ of 20 %, 50 %, 80 % and 90 % where ‘L’ is varied from 1 mm to 100 mm. It was found that above 100 mm and up to 200 mm, the MFL amplitude remains relatively constant. Each profile exhibits a similar characteristic, each being a scaled representation of the defect depth.

When ‘L’ is beyond 40 mm, the corresponding peak-to-peak amplitudes approximate a plateau, making the depth estimate consistent in this region and interpreting the depth more trivial. MFL signal amplitudes when ‘L’ is below 40 mm corresponds to the observations of Marino and Drury [25] who report the difficulty of detecting narrow or pipe type defects. One reason for this difficulty is the reduced reluctance path of the induced magnetic flux path between the closer proximity of the defect edges. The closer these edges become the lower the magnetic reluctance

becomes allowing a greater proportion of the flux to ‘jump’ directly between the two causing a reduction of MFL signal amplitude in the vicinity of the sensor.

The variability of the signal amplitudes, illustrated in Figure 1(a), as a function of defect length corroborates to an observation made by Charlton [4], “*the flux leakage magnitude was more dependent upon its area [analogous to the length in 2D] than its depth*”. Again, similar experimental results were reported by Ji et al. [26], “*as the [defect] length increases, MFL peak-to-peak will increase*”. The traits reported Charlton [4] and Ji et al. [26] can only be considered analogous to the MFL relationship in Figure 1(c) when defects are below 40 mm in length.

Figure 1(b) is an error plot depicting the difference between the actual defect depths and ones estimated from the MFL signal. In Figure 1(b), the ordinate refers to the potential deviation from the true defect depth when estimated with MFL. The deviation is derived for each of the corresponding depths in Figure 1(a) and plotted as a function of its length. This plot illustrates the potential error in the depth estimate when considering only the amplitude of the MFL signal.

An example of a reported depth error is shown by position (i), for a defect that is 10 mm in length and 90 % deep. This example demonstrates an error of up to 12 % from the true 90 % depth. This may not be a very significant error as at worst, the defect would be reported to be 78 % deep and would likely be repaired anyway. However, the example portrayed by position (ii) if unrepaired may lead to a leak before the next AST floor inspection. In this case a defect 5 mm in length and 90 % deep may be reported to be 58 % deep. Position (iii) demonstrates an imminent leak may be reported as a non-critical defect. When ‘ L ’ decreases to 1 mm and the depth is 90 %, the potential error in the reported depth can increase to 63 %, that is, a 90 % defect would be considerably under-sized and reported to be only 27 % deep. It is seen that the potential error of the depth estimate can be considerable when only the amplitude of the MFL signal is considered. Thus, by harnessing a measure of the defect length in conjunction with the conventional amplitude measure, then the profiles of Figure 1(a) could serve as a referencing scheme to translate the amplitudes of corresponding MFL signals to better estimate the true defect depth.

The next section introduces a referencing scheme based on measures presented in this section with the aim of an enhanced depth estimation, in particular those coming from narrow defects.

4. An enhanced reference map

In this section we propose an enhanced map-based defect referencing scheme, the purpose of which is to provide a more accurate depth estimate of defects located with MFL. This complete map, generated through simulation is based on the MFL amplitude profiles in Section 3 coming from a continuous range of defect lengths and including the range of depths from 20 % to 100 %.

To estimate the depth of an unknown defect, two measures from the corresponding MFL signal in conjunction with the defect reference map is required; a measure of the MFL amplitude and a measure of the defect length. These inputs are shown on Figure 2 as input 1 and input 2 respectively. Obtaining the peak-to-peak amplitude measure is relatively straight forward and to determine the defect length, we adopt the lateral peak-to-peak measure of Siebert and Sutherland [7]. Prior to assessing the enhanced defect reference map we first assess the accuracy of the adopted length measure.

The lateral peak-to-peak measure is illustrated in Figure 3(a) by means of error analysis. The error of the lateral peak-to-peak measure in *mm* is plotted against the true defect length, also in *mm*. When defects exceed 8 mm in length, the peak-to-peak measure is consistently offset by 2 mm. This offset can be overcome by normalisation. However, for defects under 8 mm, the error associated with the lateral peak-to-peak measure increases as ‘ L ’ becomes smaller. For defects below 8 mm in length, an error of 6 mm is possible, but if the consistent 2 mm is assumed and subsequently normalised then the maximum length estimate error can be reduced to 4 mm.

Figure 3(b) shows the potential error of the MFL depth estimate from defects that are 20 %, 50 %, 70 %, 80 % and 90 % deep. Each profile is a function of the defect length, varying from 0 mm and 40 mm. Two errors are considered, one estimates the defect depth using only the peak MFL amplitude measure repeated from Figure 1(b) and the second estimates the depth when the proposed reference map is used. From the amplitude only ‘dotted’ profiles in Figure 3(b), it can be seen that errors are especially high for the narrow defects, corroborating the difficult task of correctly sizing pipe type defects as reported by both Ramirez [12] and Qi [2]. However, utilising information from the MFL amplitude from a corresponding defect along with a measure of its length and the apriori reference map, a much

Proposed reference map, estimating the defect depth from the MFL amplitude and calculation of the defect length

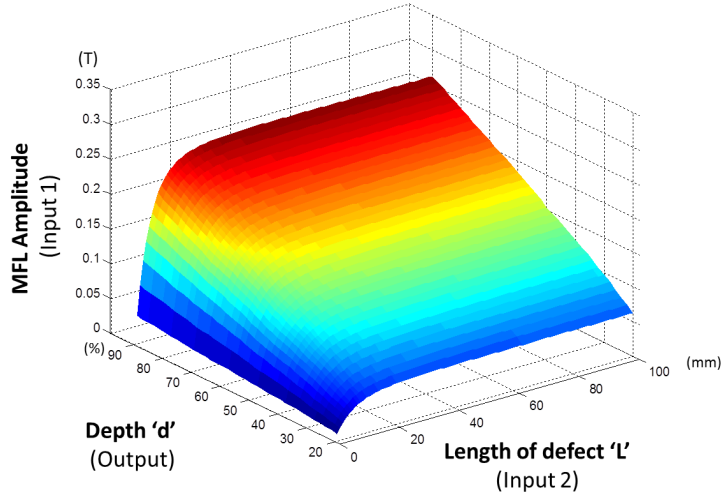


Figure 2: This enhanced reference map which could be used to estimate the depth of a defect given an MFL signal. The depth ' d ' of a defect can be estimated using the pre-determined reference map in conjunction with two input measures from the corresponding MFL signal. Input 1 can be established from the peak-to-peak amplitude of the MFL signal and input 2 is an estimate of the defects' length. The length can be obtained from the MFL signal by measuring the lateral peak-to-peak.

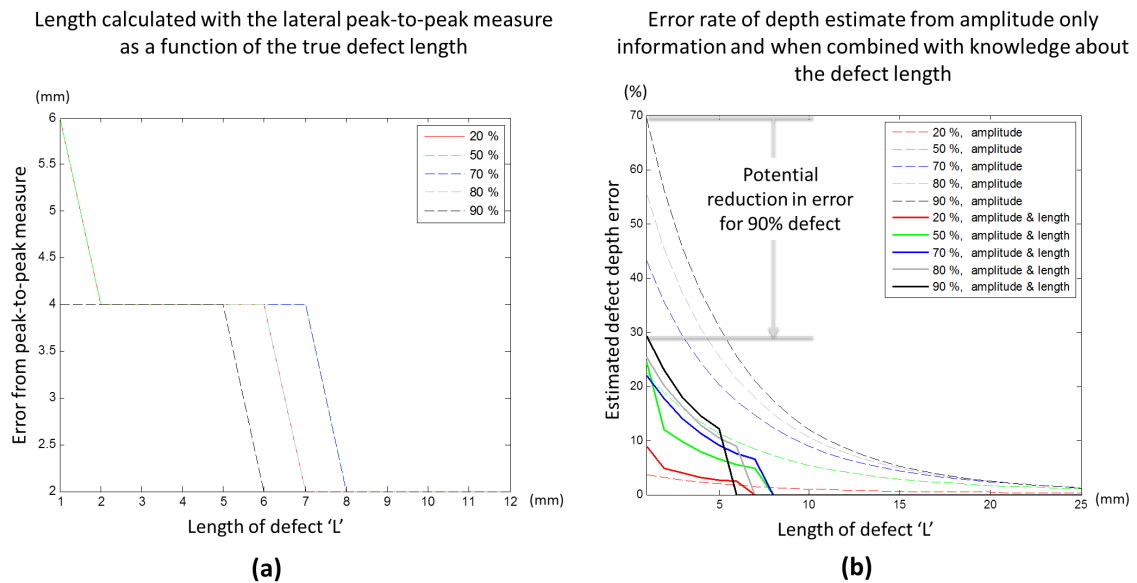


Figure 3: (a): Error analysis of the lateral peak-to-peak measure proposed by Siebert and Sutherland [7] for narrow defect lengths. Five overlapping profiles of defects with depths 20 %, 50 %, 70 %, 80 % and 90 % illustrate ambiguity between pk-pk estimates as the depth of the defect is varied. When $L > 8$ mm, the error remains constant at 2 mm. (b): Estimated depth error with MFL as a function of ' L '. For the convenience of the reader, the dotted profiles are replicated from Figure 1(b). A reduced error rate in the depth estimate can be observed when incorporating information about the MFL amplitude, the defect length and the proposed reference map. Again, the lateral peak-to-peak measure is used to estimate the length of the defect.

reduced error is possible (the solid profiles in Figure 1(b)). The nature of this enhanced approach is a consequence of the errors attributed by the sub-optimal length measure. But even with this sub-optimal length measure, the enhanced referenced map reduces the error of the defect that is 90 % deep and 1 mm in length by around 40 %, i.e. from the amplitude only 27 % to the reference map estimate of around 63 %; a defect that would certainly warrant further examination.

5. Conclusion

MFL is a rapid and robust approach that continues to be widely used to detect corrosion defects in applications where large areas are to be inspected in relatively short time scales. Once a defect has been detected, the main failing of the MFL approach is its inability to accurately size and classify. To improve sizing accuracy, defect characteristics need to be quantified with greater accuracy with the ultimate goal to map MFL signals back to their corresponding defect shapes. However, MFL signals from a narrow, *pipe* type defect remain difficult to classify.

Current practice for rapid defect characterisation can be performed via a reference map. One example of reference mapping comes from the relationship between the amplitude of MFL signals and defects that grow uniformly in both length and depth; following the trend of natural corrosion. However, the narrow pipe type defects do not exhibit the uniform growth characteristic of natural corrosion. With this in mind, a new and enhanced reference map has been proposed that, along with the MFL amplitude and information about the defect length would allow a better depth estimation.

In this paper, the lateral peak-to-peak measure suggested by Siebert and Sutherland [7] is adopted to estimate the length of defects from an MFL signal. It is shown here to be a sub-optimal measure for the narrow pipe type defects. However, the proposed reference map in conjunction with the length estimate can achieve a substantial reduction in the error of the depth estimate. An example defect that is 90 % deep in reality and would otherwise be reported to be just 27 %, following the approach presented here would be reported to be 63 %, a depth that certainly warrants further investigation in the field. An improvement to this measure requires a length measure that is suited towards narrow defects. The proposed map is considered a first step that could include additional defect features, characteristics or useful knowledge to make a more comprehensive referencing strategy.

Acknowledgements

This work is funded by Silverwing UK Ltd.

References

- [1] D. H. Saunderson. The MFE tank floor scanner - a case history. *IEE colloquium on non-destructive evaluation*, 1988.
- [2] J. Qi. Experimental study of interference factors and simulation on oil-gas pipeline magnetic flux leakage density signal. *International conference on mechatronics and automation*, 2007.
- [3] N. B. Cameron. Recommended practice for magnetic flux leakage inspection of atmospheric storage tank floors. *Health and safety executive UK*, 2006.
- [4] P. C. Charlton. A theoretical and experimental study of the magnetic flux leakage method for the analysis of corrosion defects in carbon steel plate. *PhD Thesis, Swansea institute of higher education*, 1995.
- [5] P. C. Charlton and J. C. Drury. The high speed inspection of bulk liquid storage tank floors using the magnetic flux leakage method. *Insight*, 35, No. 4:169–172, 1993.
- [6] J. C. Drury. Magnetic flux leakage technology. Available at: http://www.silverwinguk.com/ndt_technical_papers.aspx, (3/8/2011).
- [7] M. A. Siebert and J. E. Sutherland. Application of the circumferential component of magnetic flux leakage measurement for in-line inspection of pipelines. *NACE International*, 1999.
- [8] S. Huang, L. Li, H. Yang, and K. Shi. Influence of slot defect length on magnetic flux leakage. *Journal of Materials Sciences & Technology*, 20, 2004.
- [9] J. Qi, S. Qingmei, L. Nan, Z. Paschalis, and W. Jihong. Detection and estimation of oil-gas pipeline corrosion defects. *Proceedings of the 18th international conference on systems engineering (ICSE 2006)*, pages 173–177, 2006.
- [10] S. Saha, S. Mukhopadhyay, U. Mahapatra, S. Bhattacharya, and G.P. Srivastava. Empirical structure for characterizing metal loss defects from radial magnetic flux leakage. *NDT & E International*, 43:507–512, 2010.
- [11] A. R. Ramirez, N. R. Pearson, and J. S. D. Mason. An holistic approach to automatic classification of steel plate corrosion defects using magnetic flux leakage. *17th World conference on nondestructive testing (WCNDT)*, 25–28 Oct 2008.
- [12] A. R. Ramirez. Automatic classification of defects in aboveground storage tanks via magnetic flux leakage. *PhD Thesis, Swansea University*, 2009.

- [13] A. Sadr and S. Ehteram. Intelligent defect recognition from magnetic flux leakage inspection. *The e-journal of nondestructive testing*, May 2008.
- [14] A. R. Ramirez, N. R. Pearson, and J. S. D. Mason. Automatic classification of defects in a corrosion environment. *EUROCORR*, 2009.
- [15] Y. Lijian, L. Gang, Z. Guoguang, and G. Songwei. Oil-gas pipeline magnetic flux leakage testing defect reconstruction based on support vector machine. *2nd International conference on intelligent computation technology and automation.*, 2009.
- [16] P. Ramuhalli, L. Upda, and S. S. Upda. Neural network based inversion algorithms in magnetic flux leakage nondestructive evaluation. *Journal of applied physics*, 93(10), 2003.
- [17] K. C. Hari, M. Nabi, and S. V. Kulkarni. Improved fem model for defect-shape construction from mfl signal by using genetic algorithm. *Science, Measurement & Technology, IET*, July 2007.
- [18] M. Yan, S. Upda, S. Mandayam, Y. Sun, P. Sacks, and W. Lord. Solution of inverse problems in electromagnetic NDE using finite element methods. *IEEE transactions on magnetics*, 34 (5), September 1998.
- [19] C. Mandache and L. Clapham. A model for magnetic flux leakage signal predictions. *Journal of Physics D: Applied Physics*, October 2003.
- [20] M. Ravan, R.K. Amineh, S. Koziel, N.K. Nikolova, and J.P. Reilly. Three-dimensional defect reconstruction from mfl signals using space mapping optimisation. *13th International Symposium on Antenna Technology and applied electromagnetics and the Canadian radio sciences meeting*, 2009.
- [21] X. Yuan, C. Wang, X. Zuo, and S. Hou. A method of 2D defect profile reconstruction from magnetic flux leakage signals based on improved particle filter. *Insight*, 53(3), March 2011.
- [22] P. Ramuhalli, L. Upda, and S. S. Upda. Electromagnetic NDE signal inversion by function approximation neural networks. *IEEE transactions on magnetics*, 38, 2002.
- [23] A. Joshi, L. Upda, S. Upda, and A. Tamburrino. Adaptive wavelets for characterising magnetic flux leakage signals from pipeline inspections. *IEEE transactions on magnetics*, 42, 2006.
- [24] J. Fengzhu, W. Changlong, Z. Xianzhang, H. Songsshan, and L. Siyang. LS-SVM based reconstruction of 3-D defect profile from magnetic flux leakage signals. *Insight - Non-Destructive Testing and Condition Monitoring*, 49(9), 2007.
- [25] A. Marino and J. C. Drury. A comparison of the magnetic flux leakage & ultrasonic methods in the detection & measurement of corrosion pitting in ferrous plate & pipe. *15th World Conference on Non-Destructive Testing (WCNDT)*, 2000.
- [26] F. Ji, C. Wang, S. Sun, and W. Wang. Application of 3-D FEM in the simulation analysis for mfl signals. *Insight*, 51 (1), January 2009.